JOURNAL OF GEOPHYSICAL RESEARCH, VOL. 114, E08006, doi:10.1029/2009JE003334, 2009

An estimate of the terrestrial influx of large meteoroids from infrasonic measurements

Elizabeth A. Silber,[1,2] Douglas O. ReVelle,[3] Peter G. Brown,[1] and Wayne N. Edwards[1]

Received 15 January 2009; accepted 7 May 2009; published 28 August 2009.

[1] The influx rate of meteoroids hitting the Earth is most uncertain at sizes of ~10 m. Here we make use of historical data of large bolides recorded infrasonically over a period of 13 years by the U.S. Air Force Technical Applications Center (AFTAC) to refine the terrestrial influx rate at these sizes. Several independent techniques were applied to these airwave data to calculate bolide kinetic energies. At low energies our flux results are within a factor of two in agreement with previous estimates. For 5–20-m diameter objects, however, our measurements of the cumulative number of Earth-impacting meteoroids are as much as an order of magnitude higher than estimates from telescopic surveys of near-Earth objects and satellite-detected bolides impacting the Earth. The precise cause of this disagreement is unclear, though we propose several possible explanations. From our infrasound study, our best estimate for the cumulative annual flux of impactors with energy equal to or greater than E (in kilotons of TNT equivalent) is $N = 4.5\ E^{-0.6}$.

Citation: Silber, E. A., D. O. ReVelle, P. G. Brown, and W. N. Edwards (2009), An estimate of the terrestrial influx of large meteoroids from infrasonic measurements, *J. Geophys. Res.*, *114*, E08006, doi:10.1029/2009JE003334.

1. Introduction

[2] The flux of meter-sized to tens-of-meters-sized meteoroids in near-Earth space is poorly known. It is near this size threshold (below 100 m) where impactors may penetrate the atmosphere and crater the Earth's surface [*Bland and Artemieva*, 2003] and where impact effects may result in localized climate perturbations [for comparison, see *Toon et al.*, 1997]. More generally, the flux of meter-class meteoroids is critical to dating young planetary surfaces and understanding the delivery mechanisms of meteoroids from the main asteroid belt, as, for example, it is in the size range of meters to tens of meters where the Yarkovsky drift effect is most significant [*Farinella et al.*, 1998]. The most comprehensive measurement of the meteoroid flux in this size range to date by *Brown et al.* [2002] examined satellite data of light flashes produced by the disintegration of meter-sized objects in the Earth's atmosphere. This analysis, however, was dependent on assumptions about both the spectral distribution and efficiency of light production which are uncertain. More recently, *Harris* [2008] has produced estimates of the flux of 10 m and larger near-Earth objects from telescopic survey data. The new *Harris* [2008] analysis suggests a dip of as much as 1 order of magnitude in the population relative to a constant power law extrapolation (as presumed by *Brown et al.* [2002]) in the few tens to 100-m size range. Both of these studies have (generally different) built-in assumptions which would make another, independent estimate of the flux in this size regime desirable.

[3] Here we make use of the acoustic waves produced by large meteoroid impacts over a 13-year study period to estimate the influx rate for meter-sized and larger meteoroids. Meteoroid impacts produce infrasound, low-frequency acoustic waves below the frequency threshold of human hearing (~20 Hz) and above the Brunt-Vaisala frequency of the atmosphere ~10^{-3} Hz. These waves are of special interest as attenuation in the atmosphere at these frequencies is low, and hence the waves can be detected over large distances, approaching global scales at the lowest frequencies corresponding to large explosive sources. It is also possible to estimate the source energies for fireballs using acoustic records alone [*Ceplecha et al.*, 1998]. Our data set consists of historical detections of airwaves from 10 large fireballs made by a global network of microbarometers operated by the U.S. Air Force Technical Applications Center (AFTAC) covering the period from the early 1960s until the mid-1970s. This data set has been previously analyzed in part by *Shoemaker and Lowery* [1967] and in complete form by *ReVelle* [1997, 2001] for the purpose of measurement of meteoroid influx rates. The current study differs from these earlier works in that we have digitized all the original hardcopy records, corrected the cylindrical pen recordings to linear scales, applied instrument responses to the airwave signals, and remeasured all signal quantities. We note that the major remaining unknown response correction is for windpipe filtering. Here we reexamine the signal processed records estimating yields using the original period approach of *ReVelle* [1997] and independently apply a recent energy-amplitude relation derived

[1]Department of Physics and Astronomy, University of Western Ontario, London, Ontario, Canada.
[2]Formerly E. A. Sukara.
[3]EES-2, Atmospheric, Meteorological Modeling Team, Climate and Environmental Dynamics Group, Los Alamos National Laboratory, Los Alamos, New Mexico, USA.

0148-0227/09/2009JE003334$09.00

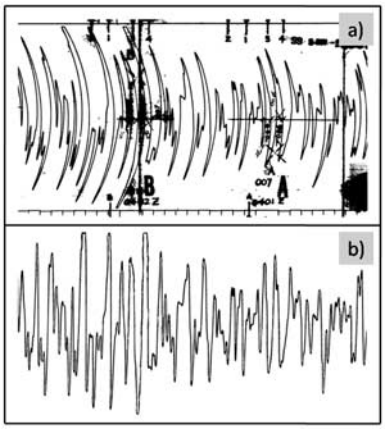

Figure 1. Channel 1, 2 November 1960: A representative example of the segment of the raw waveform (a) as scanned from the original paper record and (b) cleaned and straightened (corrected for the cylindrical pen) corresponding segment of the waveform. At this point, the cleaned and straightened waveform is subjected to further processing in order to produce a final, digitized waveform which is as close as possibly attainable to the original one.

from simultaneous satellite-infrasound measurements [*Edwards et al.*, 2006].

[4] Each infrasonic array consisted of a minimum of four microbarometer pressure sensors (channels), placed approximately 6–12 km apart, with two distinct passbands: (1) infrasonic wave band, high frequency (HF), 3 dB down at 0.04 to 8.2 Hz and (2) internal gravity wave band, low frequency (LF), 3 dB down at periods of 440–44 s [*ReVelle et al.*, 2008]. The global network of these stations was designed to detect large nuclear explosions anywhere on the planet; hence this design is well-suited to global fireball monitoring. The AFTAC-operated network differs from the currently established International Monitoring System (IMS) (which is under the umbrella of the Comprehensive Nuclear-Test-Ban Treaty (CTBT) commission) in several respects, such as the setup, sampling rates, noise processing, array element separations, and signal processing. For example, the AFTAC-operated network utilized infrasonic arrays with a large separation of sensor elements (6–12 km) compared to the IMS network (1–3 km) and a comparably lower signal-to-noise ratio compared to the IMS network. The complete AFTAC setup was geared toward monitoring and detections of large nuclear explosions, predominantly occurring in the atmosphere and yielding low-frequency infrasound, while the IMS network is designed to detect lower-yield explosions underground as well as in the atmosphere with a correspondingly higher infrasonic frequency range. In short, the historical infrasonic records that come from the AFTAC-operated network are profoundly unique and fundamentally different from those coming from the presently operated IMS network. More details of the AFTAC network, areal coverage, and instruments can be found in the work of *ReVelle* [1997]. Our current analyzed data set consists of HF detections only, although the LF data exist and were fully digitized as well.

[5] We note that this data set is unique in that it covers a long time period (13.67 years) and has several large energy events, the detection of which sets useful limits to the influx for larger (10 m) meteoroids. One event is of particular interest; it occurred off the coast of South Africa on 3 August 1963, originally estimated by *ReVelle* [1997] at ~1100 kt TNT (1 kt TNT = 4.185×10^{12} J). Our flux values will necessarily be lower limits, as not all fireball events detected by the AFTAC network have been made available for analysis, and only relatively deeply penetrating fireballs produce significant infrasound.

2. Reduction Methods and Analysis

[6] All original waveforms were recorded to strip-chart paper as well as on magnetic tape at the time of observation, with events being identified in real time by station operators who noted increased cross correlation among a given station's microbarometers. A total of 10 events were identified as being fireballs, 9 of them with a certain confirmation by other techniques, such as seismic and VLF [*ReVelle*, 1997]. The only event that did not have confirmation by any other technique is the South African event of 3 August 1963.

[7] These original chart paper records were scanned in.tiff format. Even though the scans were saved in high resolution, they were not in a suitable state for data digitization, as the original records were contaminated with various markings, such as stamps, smudges, handwritten measurements, and dates, all entered by the equipment operators. In almost all cases these markings were directly on top of a waveform, impairing the clarity of the signal; hence, a careful image cleaning was necessary to proceed to the next step. It is important to note that these scanned waveforms are very large in size (up to 84,000 pixels), limiting the choice of image manipulation software which would be capable of efficiently handling the cleanup procedure. For this purpose we used the open LINUX software program Gimp, as it can facilitate large file handling and seamless computer resource management (all raw waveforms are available at http://aquarid.physics.uwo.ca/infra_pub/2009je003334/Supplemental_material/).

[8] Once cleaned, the images were saved in their native form (.tiff) for archiving and further processing. Several Matlab programs were written for postprocessing. For example, it was necessary to correct for the cylindrical pen and "straighten" the signal for all records except for events recorded in 1971 and 1972, as those were already recorded digitally. Figure 1 shows a representative example of the raw waveform as scanned from the paper record and the corresponding example of this "straightening" for channel 1 of the 2 November 1960 event. The final stages of the process generated fully digitized waveforms which are identical to that of the scanned original. Once this was achieved, the calibration based on the original paper records was applied to each waveform. This calibration consisted of three main components: (1) the gain-setting correction, (2) the amplitude scaling, and (3) the sampling rates. An example of the finalized fully digitized and calibrated waveform for channel 1 of the 2 November 1960 event is shown in Figure 2.

[9] From these digitized records, we verified that the original measurements made by *ReVelle* [1997] were reproducible to within pen-width uncertainty which (with the

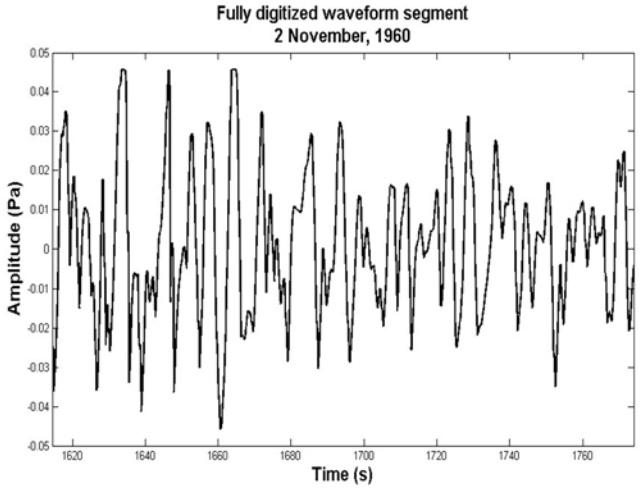

Figure 2. A fully digitized waveform of the 2 November 1960 event, channel 1: this is the same segment as in Figure 1, now fully digitized and calibrated.

exception of some transcription errors) was generally found to be the case (Table 1 contains all measurements of the original digitized and calibrated waveforms). The digital waveforms then had the instrument response of the microphones applied [*Flores and Vega*, 1975], and a final best estimate for the original waveform was produced.

[10] Figure 3 shows an example of this process and the instrument response function. The period at the maximum amplitude of the signal and peak-to-peak amplitude were measured on both the instrument-response-corrected and original waveforms for all station channels.

[11] To apply the empirical yield relation from *Edwards et al.* [2006], it is desirable to know the wind conditions between the source and receiver at the time of the event. Since these events all occurred at a time before upper wind measurements were globally available (except for the NASA rocket grenade network), we could only perform statistical averages of the wind from more recent years data over the same great circle paths from the U.K. Meteorological Office (UKMO) model atmosphere [*Swinbank and O'Neill*, 1994] to estimate the original stratospheric wind field. However, we find that the average wind values are often smaller than their standard deviations, making wind corrections almost meaningless. We choose instead to use these amplitude relations without wind corrections with the understanding that this will necessarily produce greater uncertainty in the final energy estimates. We note, however, that for very large events, the previous work by *Edwards et al.* [2006] shows the wind corrections to be relatively minor for the largest energy events, and since most of our fireballs fall into the large energy category as defined by *Edwards et al.* [2006], we expect the impact of this simplification to be minor in most cases.

3. Estimating Source Energies for Fireballs

[12] Estimating the source energy for a large impulsive atmospheric infrasonic source generally relies on empirical relations derived from sources with known provenance. Among these, the most often cited for fireballs is the relation first introduced by *ReVelle* [1997], derived from infrasonic measurements of ground level nuclear explosions recorded by AFTAC. These relations make use of the period at maximum amplitude, which is generally more insensitive to propagation effects than amplitude only.

[13] These relations are

$$\log(E/2) = 3.34\log(P) - 2.58 \qquad E/2 \leq 100\text{kt} \tag{1}$$

$$\log(E/2) = 4.14\log(P) - 3.61 \qquad E/2 \geq 40\text{kt} \tag{2}$$

Here, E is the total energy of the event (in kilotons of TNT), P is the period (in seconds) at maximum amplitude of the waveform, and the factor 1/2 is present because these relations were originally derived for nuclear explosions, where 50% of the source energy was presumed lost into radiation.

[14] Most recently, *Edwards et al.* [2006] examined a large number of fireballs detected simultaneously with infrasound and by satellite measurements and found

$$E = 10^{3(0.0018v_h - 2.58)/1.35} R^3 A^{3/1.35} \qquad E > 7kt \tag{3}$$

$$E = 10^{3(0.0177v_h - 3.36)/1.74} R^3 A^{3/1.74} \qquad E < 7kt \tag{4}$$

where E is the energy yield of a bolide (in tons of TNT) (presumed to be larger than 7 kt TNT in equation (3) and less than 7 kt TNT in equation (4)), R is the range to the bolide (in km), A is the maximum peak-to-peak amplitude (in Pa), and v_k is the source-receiver wind speed (in m/s). Since it is unclear which of these relations is most applicable to fireballs, we use all approaches in section 4 to derive energy and recurrence intervals.

4. Results and Discussion

[15] We performed several energy calculations on digitized original and response-function-corrected waveforms, including applying the original AFTAC relations (1) and (2) and the empirical relation equations (3) and (4) [*Edwards et al.*, 2006]. As previously mentioned, all events, except for the 3 August 1963 event, were reliably detected by methods and instruments [*ReVelle*, 1997] other than just infrasound. For the 3 January 1965 event, because the signal is concentrated at such a high acoustic frequency where the relationship between period and yield is less sensitive to meteorological conditions and the range is very low, the yield is believed to be known most reliably of all the events in our data set. This event was subsequently used as a check on the AFTAC energies to scale all other events by adding a correction factor to the AFTAC period relation (1). This method reduced kinetic energy estimates of the corrected waveforms by approximately one half, but did not produce a significant change to the slope of the cumulative number versus energy meteoroid flux profile.

[16] There are 14 distinct AFTAC stations included in the data we have used. Generally, few explosions are recorded by many stations, particularly at lower energies. This is because the propagation and detection of infrasound

Table 1. Summary of All Ten Bolide Events From the Historical Data Set, Sorted by Date[a]

Event Date	Channel	Digitized Peak-to-Peak Amplitude (Pa)	Digitized Period at Maximum Amplitude (s)	Digitized Period Standard Deviation (s)
3 August 1963	JB-1	0.23	35.29	1.83
3 August 1963	JB-2	0.15	25.49	1.05
3 August 1963	JB-3	0.16	25.49	1.05
3 August 1963	JB-4	0.14	25.49	1.05
3 August 1963	PB-1	0.21	40.51	2.10
3 August 1963	PB-2	0.23	37.55	1.01
3 August 1963	PB-3	0.19	37.24	5.70
3 August 1963	PB-4	0.29	46.71	4.89
31 March 1965	MF-1	0.20	15.44	1.67
31 March 1965	MF-2	0.21	15.72	2.45
31 March 1965	MF-3	0.21	11.27	1.97
31 March 1965	MF-4	0.20	15.24	1.05
31 March 1965	PD-1	1.23	13.86	1.32
31 March 1965	PD-2	0.65	13.12	1.68
31 March 1965	PD-3	1.76	14.40	1.63
31 March 1965	PD-4	1.75	13.28	1.52
12 June 1966	FH-1	0.12	8.59	1.13
12 June 1966	FH-2	0.12	6.79	0.34
12 June 1966	FH-3	0.10	7.37	0.27
12 June 1966	FH-4	0.12	7.99	1.04
12 June 1966	GE-1	0.11	11.70	0.80
12 June 1966	GE-2	0.11	8.47	0.84
12 June 1966	GE-3	0.11	9.48	0.97
12 June 1966	GE-4	0.06	10.59	1.07
12 June 1966	MF-1	0.06	7.98	2.17
12 June 1966	MF-2	0.07	6.45	0.64
12 June 1966	MF-3	0.06	7.96	0.95
12 June 1966	MF-4	0.06	7.36	0.43
12 June 1966	RW-1	0.24	6.63	0.55
12 June 1966	RW-2	0.27	7.06	0.45
12 June 1966	RW-3	0.25	6.78	0.07
12 June 1966	RW-4	0.28	6.60	0.51
14 April 1972	GE-1	0.53	8.48	1.27
14 April 1972	GE-2	0.10	8.77	0.20
14 April 1972	GE-3	0.20	8.63	0.42
14 April 1972	GE-4	0.14	6.65	0.72
14 April 1972	FH-1	0.07	7.33	2.39
14 April 1972	FH-2	0.02	6.87	0.99
14 April 1972	FH-3	0.10	9.03	2.31
14 April 1972	FH-4	0.13	7.46	2.64
14 April 1972	GK-1	0.49	13.18	3.43
14 April 1972	GK-2	0.49	11.50	0.50
14 April 1972	GK-3	0.69	14.29	0.22
14 April 1972	GK-4	0.59	12.83	2.23
14 April 1972	GS-1	0.19	21.06	3.80
14 April 1972	BO-1	1.27	15.36	1.70
14 April 1972	BO-2	1.21	10.20	1.32
14 April 1972	BO-3	0.60	11.82	0.44
14 April 1972	BO-4	0.28	9.84	4.27
2 November 1960	TD-1	0.24	8.23	0.91
2 November 1960	TD-2	0.23	9.98	3.65
2 November 1960	TD-3	0.16	7.98	1.64
2 November 1960	TD-4	0.22	9.84	3.83
26 September 1962	SS-1	0.09	12.84	1.20
26 September 1962	SS-2	0.06	17.76	2.21
26 September 1962	SS-3	0.11	27.47	3.15
26 September 1962	SS-4	0.06	8.73	1.70
27 September 1962	DC-1	0.59	8.89	0.99
27 September 1962	DC-2	0.66	16.49	3.20
27 September 1962	DC-3	0.48	9.21	0.73
27 September 1962	DC-4	0.50	13.36	5.73
30 November 1964	PB-1	0.54	6.89	1.18
30 November 1964	PB-2	0.42	8.55	0.40
30 November 1964	PB-3	0.23	8.26	0.92
30 November 1964	PB-4	0.33	7.80	1.26
3 January 1965	KP-1	0.12	5.38	1.24
3 January 1965	KP-2	0.15	6.02	0.91
3 January 1965	KP-3	0.12	4.76	0.18
3 January 1965	KP-4	0.12	4.71	1.22
8 January 1971	TT-4	0.06	9.46	0.29

[a]The data includes the measurements of the digitized and calibrated original waveforms: maximum peak-to-peak amplitude, the period at maximum amplitude, and the standard deviation of the period.

depends on signal attenuation, upper atmosphere wind conditions, time of the day, and local noise, all of which vary dramatically from site to site. For comparison, the current IMS network is designed generally to have a minimum two-station detection of a one kt explosion anywhere on Earth [*Christie*, 2007], but this is with 60 stations and modern digital instruments and signal processing. A detailed analysis of the AFTAC network sensitivity as a function of yield and wind conditions was performed by AFTAC during the operational years of the network. That system sensitivity bias is shown in Figure 4 and forms the basis for our flux corrections. Note that the probability is shown for a two-station detection where the range to the fireball would be unambiguously resolved with the infrasound measurements alone. We emphasize that the current fireball data set is only a portion of the total AFTAC fireball data set; some events are not included and we expect others may not have met the detection thresholds discussed earlier. As such, our flux values should be considered lower limits.

[17] The total collection duration of the AFTAC network was 13.67 years, and using the percent coverage of Earth (Figure 4) as a function of yield, season, and hemisphere [*ReVelle*, 1997], we computed an equivalent time-area collection product, which together with our infrasound-derived source energies produces an equivalent meteoroid flux at the Earth. Our final results are shown in Figure 5. Note that the range to each event is determined by the great circle intersections from two or more stations: range errors are typically of the order of a few hundred kilometers at most and form a negligible contribution to the overall error in flux estimation. Here we exhibit the difference between our computed influx rate using the AFTAC period relation and the empirical source energy estimate from *Edwards et al.* [2006] appropriate to each event depending on whether it had $E > 7$ kt or $E < 7$ kt. Note that we include for comparison various other flux estimates from telescopic surveys of near-Earth objects, satellite measurements of fireball light flashes in the Earth's atmosphere, and scaling from lunar crater statistics. The errors for our measurements are shown for each point and reflect counting statistics (error in ordinate) as well as the standard deviation in measured energy due to station and individual channel differences (error in abscissa).

[18] Events recorded by two or more stations generally show noticeable variations in estimated energy: this may be due to the source shock wave originating from different locations along a bolide's trajectory, variations in meteorological conditions along differing source-receiver paths, and

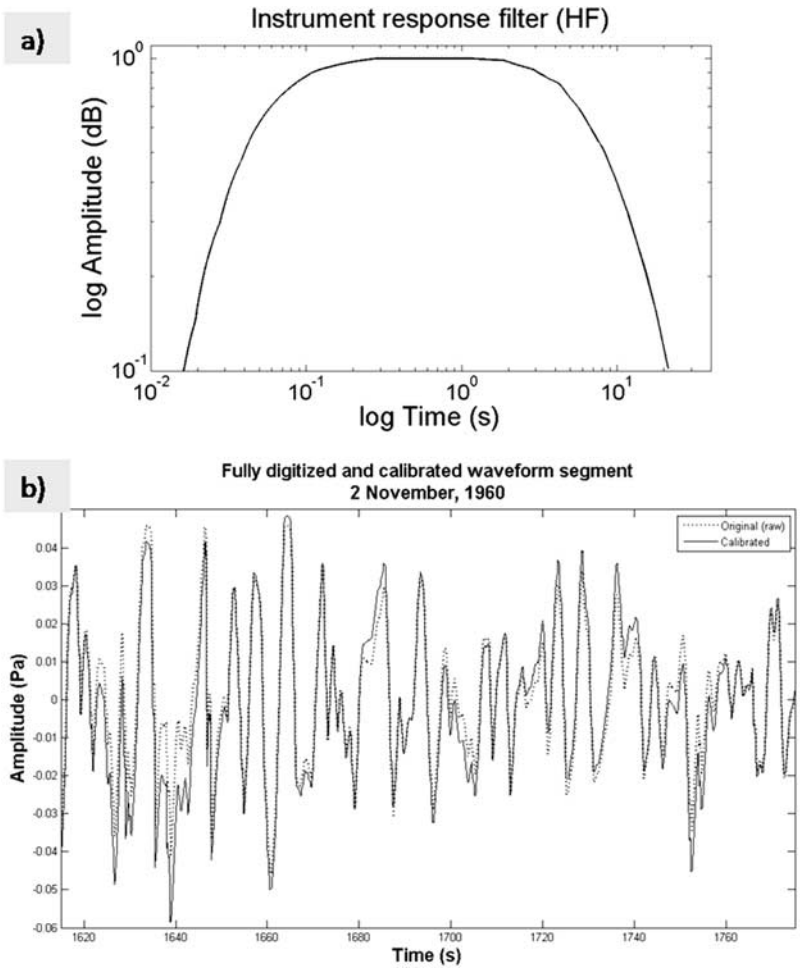

Figure 3. (a) The frequency response function adopted from *Flores and Vega* [1975], with 3 dB down between 0.04–8.2 Hz; (b) the original digitized (dotted line) and corrected waveforms (solid line) superimposed.

factors such as local noise and seasonal variations. Consequently, these events are averaged across all stations and channels to give a singular kinetic energy estimate (Table 2) per event. We have also computed the mean infrasonic signal speeds between the bolides and each receiving station for which we have location information and find the signal speeds to range from 258.9–341.2 m/s, consistent with stratospheric ducting in almost all cases [for comparison, see *Ceplecha et al.*, 1998]. As stratospheric signal arrivals are presumed for both energy relations, this implies that the energy estimates are internally self-consistent.

[19] In general, the two different approaches produce flux values which are in agreement within error. It is notable that the flux estimates agree best with all other techniques in the lower energy ranges (a few kilotons and smaller) where number statistics are the best. However, the significant feature of this influx curve is the relatively high predicted impact flux at the Earth for ~10–20-m diameter objects, independent of the choice of yield relation.

[20] Caution must be exercised in interpretation at this high-energy end: only a few events contribute to each of these points, and errors in energy estimates in some cases span an order of magnitude. Among these is the Revelstoke fireball of 31 March 1965. Our energy estimates of 40–140 kt

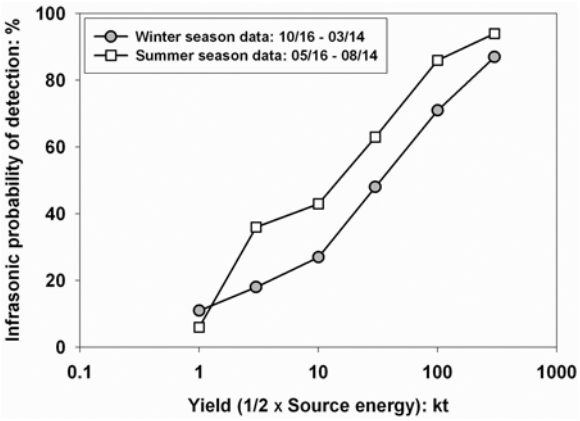

Figure 4. AFTAC: Infrasonic probability of detection as a function of yield and the time of year, derived for low-altitude nuclear explosions and with detection declared using two or more infrasonic arrays [*ReVelle*, 1997]. Winter and summer seasons are defined as 16 October to 14 March and 16 May to 14 August each year, respectively. Events falling between these dates, during times of the stratospheric wind jet transition, used interpolated versions of the probability.

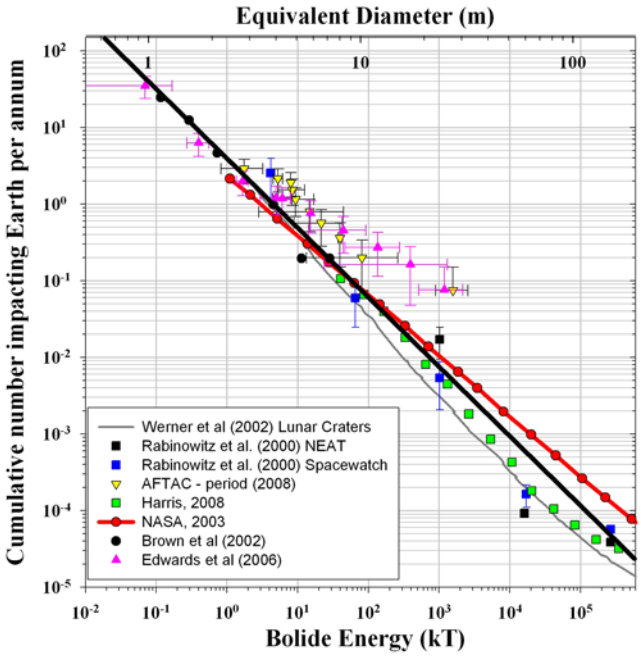

Figure 5. Cumulative influx curve showing data from a global debiasing of all telescopic surveys [*Harris*, 2008] and from individual detailed debiased flux values from the Spacewatch and NEAT programs [*Rabinowitz et al.*, 2000]. Also shown are the equivalent impact flux inferred from lunar-cratering data [*Werner et al.*, 2002] and from satellite-observed bolide impacts in the atmosphere [*Brown et al.*, 2002] as well as the power law fit and extrapolation for these data (solid black line with N = 3.7 $E^{-0.90}$). The NASA 2003 Near-Earth Object (NEO) Science Definition Team report estimated flux is shown and is well represented by a relationship of N = 2.4 $E^{-0.79}$ [*Stokes et al.*, 2003]. Note that this power law is an extrapolation from larger (kilometer-sized) NEOs. Our two new sets of data points from the digitized historic bolide data set using (1) the AFTAC energy-period relation [*ReVelle*, 1997] using periods derived in this work (labeled AFTAC period 2008) and (2) the empirical relation using signal amplitudes [*Edwards et al.*, 2006] are shown for comparison.

are order-of-magnitude consistent with those of *Shoemaker* [1983] who suggested 20 kt and *ReVelle* [2007] whose entry modeling predicts an energy of 13 kt. Most critical to the flux at the high end is the energy estimate for the 3 August 1963 bolide, the most energetic event in this data set. Depending on the method used, source energies range from 540–1990 kt, which broadly agrees with the recent estimate of 1100 kt [*ReVelle*, 1997]. *Shoemaker* [1983] estimated this event to have an energy of 500 kt, while *Edwards et al.* [2006] found an energy of 270 ± 90 kt; both of these earlier estimates used the instrumentally uncorrected waveforms, having smaller amplitudes and lower periods than the corrected versions we employed, and hence are extreme lower limits. Even accounting for possible uncertainties due to upper air winds and variations in the observed period of the waveforms, the extreme lower bound for this event is >300 kt. The nature of this one bolide remains a mystery; no other reports exist of the effects of this large impact (as may be expected of an event occurring far from land in this time period), and unlike most other events in the AFTAC database, this one did not have independent confirmation from other techniques. It remains possible that this event was not a bolide but rather another source.

[21] The discrepancy in the infrasonically estimated flux at the 5–20-m size range may reflect a systematic overestimation in source energies by our two different techniques; neither has been calibrated with bolides at these high energies, so we are extrapolating from lower bolide energy estimates for the amplitude estimates and from nuclear tests for the AFTAC case. Furthermore, seasonal variations play a significant role in efficiency of signal propagation and detection, with the summer season preferentially producing lower energy estimates. Alternatively, the infrasonic measurements may be detecting an impacting population of objects not easily seen telescopically, perhaps with low albedos. The order-of-magnitude difference in apparent flux rates in this case could reflect a large population of darker objects. The differences in the slopes of the distributions are harder to explain unless asteroid albedos change substantially over a very small size range, a situation we view as improbable. Satellite data, however, are also most consistent with the telescopic flux numbers in slope and magnitude and would not be obviously biased in the same way as telescopic measurements by albedo properties alone. Using these two energy scales, if we presume the influx follows a power law (which is only very crudely correct), over our observed size range we find

$$N = 4.05^{+0.56}_{-0.49} E^{-0.578\pm0.034} \quad (5)$$

$$N = 4.49^{+0.95}_{-0.79} E^{-0.603\pm0.055} \quad (6)$$

for the empirical yield and AFTAC-period approaches, respectively. Here N is the cumulative number of objects hitting the Earth per annum and E is the energy in kilotons TNT equivalent. These relations predict approximately one 11–12 kiloton (or larger) impact globally per annum, roughly a factor of 2–3 higher in energy than other techniques. Our relations predict a megaton event once every ~15 years, approximately 5–10 times more frequently than telescopic surveys suggest.

5. Conclusions

[22] We have presented new estimates for the flux of meter-sized to tens-of-meters-sized objects impacting the Earth based on acoustic recordings made by the AFTAC infrasound network during the period from the early 1960s until the mid-1970s. We have digitized and applied corrections to the original paper analog infrasonic records of ten large fireballs and then applied several different yield relations to estimate the kinetic energy of each event. From these energy estimations and coverage estimates of the original AFTAC network, we have estimated the global meteoroid influx of meters to tens of meters sizes. Our findings suggest a shallower slope of cumulative number versus energy than is found from either satellite-observed fireball flashes in the terrestrial atmosphere or fluxes inferred from telescopic surveys.

Table 2. Summary of All Ten Bolide Events From the Historical Data Set, Sorted by Date[a]

Date	Station	Back Azimuth (deg)	Great Circle Range (km)	Signal Velocity (m/s)	AFTAC Period- Energy Relation (kt)	Empirical Relation (kt)
2 November 1960	TD	n/a	4004.0	306.1	$8.4135^{+4.1454}_{-3.0770}$	$4.9549^{+2.5382}_{-1.9753}$
26 September 1962	SS	173.0	1112.0	294.2	$81.2511^{+179.5343}_{-67.9152}$	$0.0677^{+0.1004}_{-0.0590}$
27 September 1962	DC	118.7	872.7	303.0	$14.7872^{+11.9476}_{-29.6139}$	$0.4039^{+0.1514}_{-0.1306}$
3 August 1963	JB	170.0	11282.1	298.0	$930.2768^{+453.0749}_{-337.3165}$	$1182.8468^{+983.2660}_{-665.9478}$
3 August 1963	PB	n/a	13824.0	293.5	$930.2768^{+453.0749}_{-337.3165}$	$1182.8468^{+983.2660}_{-665.9478}$
30 November 1964	PB	n/a	5219.1	312.9	$9.3240^{+7.66924}_{-4.8407}$	$44.0152^{+48.5490}_{-29.7263}$
3 January 1965	KP	84.1	3123.6	272.6	$1.7538^{+1.4832}_{-0.9263}$	$1.6695^{+0.3318}_{-0.3062}$
31 March 1965	MF	145.8	2497.7	333.0	$39.7327^{+2.3356}_{-2.2432}$	$135.3897^{+142.9545}_{-88.9490}$
31 March 1965	PD	193.8	3497.1	303.6	$39.7327^{+2.3356}_{-2.2432}$	$135.3897^{+142.9545}_{-88.9490}$
12 June 1966	FH	60.6	4828.0	n/a	$5.2929^{+0.8735}_{-0.7829}$	$6.0986^{+2.0242}_{-1.7123}$
12 June 1966	GE	77.4	6678.8	n/a	$5.2929^{+0.8735}_{-0.7829}$	$6.0986^{+2.0242}_{-1.7123}$
12 June 1966	MF	222.5	4425.7	258.9	$5.2929^{+0.8735}_{-0.7829}$	$6.0986^{+2.0242}_{-1.7123}$
12 June 1966	RW	n/a	2896.8	335.3	$5.2929^{+0.8735}_{-0.7829}$	$6.0986^{+2.0242}_{-1.7123}$
8 January 1971	TT	n/a	13892.0	n/a	8.0222	15.2560
14 April 1972	GE	220.6	3701.5	293.8	$21.5462^{+21.7458}_{-12.6370}$	$393.7589^{+917.7597}_{-369.8045}$
14 April 1972	FH	236.4	5471.8	294.2	$21.5462^{+21.7458}_{-12.6370}$	$393.7589^{+917.7597}_{-369.8045}$
14 April 1972	GK	n/a	7805.3	316.5	$21.5462^{+21.7458}_{-12.6370}$	$393.7589^{+917.7597}_{-369.8045}$
14 April 1972	BO	n/a	4345.2	341.2	$21.5462^{+21.7458}_{-12.6370}$	$393.7589^{+917.7597}_{-369.8045}$

[a]The back azimuth entered as n/a indicates this information is not published for a particular station. We include results for two methods of source kinetic energy estimation: (1) AFTAC period-energy relation [*ReVelle*, 1997], where equation (1) was applied to all bolide events except for the 3 August 1963 event and equation (2) was applied to the latter; and (2) empirical relation for $E > 7$ kt and $E < 7$ kt, where appropriate, from *Edwards et al.* [2006]. These results are based on digitized and instrument-response-corrected waveforms. For multistation events, kinetic energy is averaged across all stations and channels. Error estimates in the final energies are based on the spread in measurement errors. Signal velocities for the 12 June 1966 fireball are below that expected of stratospheric returns at two stations. It is possible either thermospheric returns or strong counterwind returns are responsible.

[23] Much of this difference is due to the very high inferred flux rate at the largest sizes produced because of inclusion of a single event, namely the 3 August 1963 fireball which occurred off the coast of South Africa. From examination of many different yield relations, application of plausible wind corrections, and accounting for uncertainties in period and amplitude measurement we conclude that this large event is plausibly in the megaton yield range, with extreme lower energy bounds of ~300 kt. If this event is removed from our data set, our inferred cumulative influx values based on the AFTAC-period relationship becomes $N = 6.5\ E^{-0.76}$, much closer to the slope of the NASA Science Definition Team study and largely in agreement within error to flux measurements made by satellite and telescopic surveys. Removal of the 3 August 1963 fireball from the curve using the *Edwards et al.* [2006] empirical relation does not change its slope significantly. While the difference in slope and intercept produced using our full data set may reflect a true difference in flux between the various recording techniques, it is also possible that this event is a statistical anomaly, a nonmeteoric event, or perhaps was of much lower energy but somehow produced a much larger acoustic signature than is typical for fireballs. From our measurements and presuming that the flux curve should follow a power law (equations (5) and (6)), we find that the largest annual impact event expected would be in that 11–12 kiloton range, several factors higher than found with other techniques. However, at the upper end, a large event of a megaton would occur on the order of every 15 years, approximately 5–10 times more than that estimated using telescopic data. The underlying cause for the disparity between these data sets, particularly at the high end, remains unclear.

[24] **Acknowledgments.** P.G.B. thanks the Natural Sciences and Engineering Research Council of Canada and the Canada Research Chairs program for funding. E.A.S. wishes to thank the U.K. Met Office for supplying the initial stratospheric assimilated data via the British Atmospheric Data Center. The authors thank Alan W. Harris (United States) for helpful comments on an earlier version of this manuscript.

References

Bland, P. A., and N. A. Artemieva (2003), Efficient disruption of small asteroids by Earth's atmosphere, *Nature*, *424*(6946), 288–291, doi:10.1038/nature01757.

Brown, P. G., R. E. Spalding, D. O. ReVelle, E. Tagliaferri, and S. P. Worden (2002), The flux of small near-Earth objects colliding with the Earth, *Nature*, *420*, 294–296, doi:10.1038/nature01238.

Ceplecha, Z., J. Borovička, W. G. Elford, D. O. ReVelle, R. L. Hawkes, V. Porubčan, and M. Šimek (1998), Meteor phenomena and bodies, *Space Sci. Rev.*, *84*(3/4), 327–471, doi:10.1023/A:1005069928850.

Christie, D. R. (2007), Recent developments in infrasound monitoring technology: Application to CTBT verification, *CTBTO Spectrum*, *10*, 18–19, 24.

Edwards, W. N., P. G. Brown, and D. O. ReVelle (2006), Estimates of meteoroid kinetic energies from observations of infrasonic airwaves, *J. Atmos. Sol. Terr. Phys.*, *68*(10), 1136–1160, doi:10.1016/j.jastp.2006.02.010.

Farinella, P., D. Vokrouhlicky, and W. K. Hartmann (1998), Meteorite delivery via Yarkovsky orbital drift, *Icarus*, *132*(2), 378–387, doi:10.1006/icar.1997.5872.

Flores, J. S., and A. J. Vega (1975), Some relations between energy yield of atmospheric nuclear tests and generated infrasonic waves, *J. Acoust. Soc. Am.*, *57*(5), 1040–1043, doi:10.1121/1.380571.

Harris, A. (2008), What Spaceguard did, *Nature*, *453*, 1178–1179, doi:10.1038/4531178a.

Rabinowitz, D. L., E. F. Helin, K. J. Lawrence, and S. H. Pravdo (2000), A reduced estimate of the number of kilometer-sized near-Earth asteroids, *Nature*, *403*, 165–166, doi:10.1038/35003128.

ReVelle, D. O. (1997), Historical detection of atmospheric impacts by large bolides using acoustic-gravity waves, *Ann. N. Y. Acad. Sci.*, *822*, 284–302, doi:10.1111/j.1749-6632.1997.tb48347.x

ReVelle, D. O. (2001), Global infrasonic monitoring of large bolides, in *Proceedings of the Meteoroids 2001 Conference, 6–10 August 2001, Kiruna, Sweden*, *ESA SP-495*, pp. 483–489, ESA Publ. Div., Noordwijk, Netherlands, ISBN:92-9092-805-0.

ReVelle, D. O. (2007), NEO fireball diversity: Energetics-based entry modeling and analysis techniques, in *Proceedings of the International Astronomical Union Symposium*, vol. 236, pp. 95–106, Cambridge Univ. Press, Cambridge, U. K., doi:10.1017/S1743921307003122.

ReVelle, D. O., E. A. Sukara, W. N. Edwards, and P. G. Brown (2008), Reanalysis of the historic AFTAC bolide infrasound database, *Earth Moon Planets*, *102*(1–4), 337–344, doi:10.1007/s11038-007-9173-3.

Shoemaker, E. M. (1983), Asteroid and comet bombardment of the Earth, *Annu. Rev. Earth Planet. Sci.*, *11*, 461–494, doi:10.1146/annurev.ea.11.050183.002333.

Shoemaker, E. M., and C. J. Lowery (1967), Airwaves associated with large fireballs and the frequency distribution of energy of meteoroids, *Meteoritics*, *3*, 123–124.

Stokes, G. H., et al. (2003), Study to determine the feasibility of extending the search for near-Earth objects to smaller limiting diameters. Report of the Near-Earth Object Science Definition Team, 154 pp., Solar Syst. Explor. Div., Off. of Space Sci., NASA, Washington, D. C.

Swinbank, R., and A. A. O'Neill (1994), Stratosphere-troposphere data assimilation system, *Mon. Weather Rev.*, *122*(4), 686–702, doi:10.1175/1520-0493(1994)122<0686:ASTDAS>2.0.CO;2.

Toon, O. B., K. Zahnle, D. Morrison, R. P. Turco, and C. Covey (1997), Environmental perturbations caused by the impacts of asteroids and comets, *Rev. Geophys.*, *35*(1), 41–78.

Werner, S. C., A. W. Harris, G. Neukum, and B. A. Ivanov (2002), The near-Earth asteroid size-frequency distribution: A snapshot of the lunar impactor size-frequency distribution, *Icarus*, *156*, 287–290, doi:10.1006/icar.2001.6789.

P. G. Brown, W. N. Edwards, and E. A. Silber, Department of Physics and Astronomy, University of Western Ontario, 1151 Richmond Street, London, ON, N6A 3K7, Canada. (elizabeth.silber@uwo.ca)

D. O. ReVelle, EES-2, Atmospheric, Meteorological Modeling Team, Climate and Environmental Dynamics Group, Los Alamos National Laboratory, P.O. Box 1663, MS D401, Los Alamos, NM 87545, USA.